SIMULATION OF A CARDIAC CELL. Part I: AN ELECTRO-CHEMICAL MODEL

Rossany Roche[1], Rosalba Lamanna[1], Marisol Delgado[1], FranÇois Rocaries[2], Yskandar Hamam[2], FranÇoise Pecker[3]

[1]Universidad Simón Bolívar, Departamento de Procesos y Sistemas, Apartado 89000, Valle de Sartenejas, Edo. Miranda 9995, Venezuela.
[2]Groupe ESIEE, Laboratoire Algorithmique et Architecture des Systèmes Informatiques (A2SI), Cité Descartes, BP 99 93162, Noisy-Le-Grand, Paris, France.
[3]Institut National de la Santé et de la Recherche Médicale (INSERM), U581, Créteil, F-94010 France.

Recibido: octubre de 2007 Recibido en forma final revisado: febrero de 2009

ABSTRACT

A global model of the cardiac muscle cell is formulated, integrating the electrical and chemical dynamical aspects of the different components in the cytosol, the sarcoplasmic reticulum, and the cellular membrane (L-channels, Ryanodine channels, SERCA-pump, ATP-pump, Na^+-Ca^{2+}-exchanger, myofibrilles). The model is based on the idealization of the cell as a two-interconnected-stirred-tank-reactor system. It produces the expected time responses of the excitation-contraction (E-C) coupling, i.e. the oscillatory-bell-shaped curve in calcium dynamics and the characteristic plateau phase in membrane potential. Validations of the model with experimental data show that it can be adapted to represent cells of different species. Using sensitivity analysis, the phenomenological structure of the model allows the identification of the cellular sub-systems that are related to specific or altered dynamics, and hence the applications of the model in experiment design, drug-effect analysis and cardiac-pathology treatment.

Keywords: Cardiac modeling, Cardiac cell, E-C coupling, Calcium dynamics, Cellular simulation.

SIMULACIÓN DE LA CÉLULA CARDIACA. Part I: UN MODELO ELECTRO-QUÍMICO

RESUMEN

En este trabajo, se formula un modelo matemático integral de la célula del músculo cardíaco que toma en cuenta los fenómenos químicos y eléctricos que ocurren en las diversas estructuras que componen los diferentes elementos celulares: el retículo sarcoplásmico (canales de Rianodina, bomba SERCA), la membrana celular (canales L, bomba ATPasa, intercambiador Na^+-Ca^{2+}) y citosol (miofibrillas). El modelo está basado en la interpretación de la célula como dos tanques agitados e interconectados donde ocurren reacciones químicas ("two-interconnected-stirred-tank-reactor system"). Este modelo reproduce la duración del proceso de excitación-contracción ("E-C coupling") esperado, así como las formas características para la curva de la dinámica de calcio (campana asimétrica) y para la curva del potencial de membrana (potencial en forma de meseta). El proceso de validación con datos experimentales mostró que el modelo puede adaptarse para representar el comportamiento de células de diferentes especies de animales. Se realizó un análisis de sensibilidad que mostró que la estructura fenomenológica del modelo permite identificar el comportamiento de los diferentes elementos de la célula y relacionarlos de manera específica con dinámicas alteradas. Esto habilita al modelo para utilizarlo como herramienta en el diseño de protocolos experimentales, análisis de efectos de fármacos y formulación de tratamientos para cardiopatías.

Palabras clave: Modelado cardiaco, Célula cardiaca, Contracción-relajación, Dinámica de calcio, Simulación celular.

INTRODUCTION

Virtually all forms of heart disease are caused by loss or an inadequate functioning of cardiac muscle cells (cardiomyocytes). Cardiomyocytes are the base of the pumping (contraction-relaxation) movement (Stern, 1992). It is widely accepted that two interdependent aspects modulate the excitation-contraction and relaxation of the cardiac muscle cell (E-C coupling process; Tseg, 1988), namely, the cyclic changes in the cell membrane potential, and the variations in calcium concentration, due to the transport of the calcium and other ions through the cardiomyocyte membranes (Bray *et al*. 1994; Guyton, 1997).

In order to develop appropriate strategies for pharmacological therapy in heart diseases, the mechanisms underlying the E-C coupling process must be well understood. A large number of "in vitro" and "in vivo" experiments, mostly qualitatively focused, are routinely carried out in biological research to study the role of several sub-cellular elements (Gavaghan *et al*. 2006). As a consequence, the development of new drugs or treatments consumes large amounts of resources and has not yet produced a complete understanding of the cellular system.

As an alternative, a mathematical model of the cell is an excellent tool to obtain better understanding of the E-C coupling process. It also allows the substitution of an important part of laboratory experiments by "in silico" experiments or simulations. A model can be used to design experimental protocols or test new ones, to reduce experimental variations, to design alternative experiments and to discard "a priori" non-desirable drug effects.

When the model is based on physical and biochemical laws, it also helps us to understand the role of the different cellular elements in alternative dynamic responses of the cell. Furthermore, the model can be adapted (by parametric identification; Söderström & Stoica, 1989) to different kinds of cells using specific sets of experimental data. Special identification techniques allow not only the embedding of experimental data into the model but also the embedding of expert knowledge.

The first models of the cardiac muscle cell were devoted to the description of the membrane potential (electrical models) due to the availability of patch clamp techniques allowing the measurement of ionic currents (Sakmann & Neher, 1995). The development of fluorescents methods helped to obtain specific information about calcium signalling (Bray *et al*. 1994), and was the reason why calcium homeostasis models (chemical models) were developed afterwards.

However, cardiac models have often been focused on only one aspect: the calcium dynamic or the electrical aspect, in spite of the evident relationship of the two phenomena. Therefore electrical formalism and empirical relations separately are insufficient to represent a complete E-C coupling process.

Among the electrical models, models based on the works of Luo & Rudy (1994) and Noble (2002) can be found, among others (Winslow *et al*. 1999; Jafri *et al*. 1998; Fox *et al*. 2001; Tusscher & Panfilov, 2006; Iribe *et al*. 2006). They contain a complete description of the electrophysiological aspects of the cell along with some empirical blocks, and the results have been validated using patch clamp techniques. Some of these models are packaged in the commercial tool CardioPrism® for the pharmacological industry (Zenglan, 2001). Generally, they reproduce typical membrane potential, but give a very fast calcium dynamic cycle (300-400 ms) which does not agree with the cardiomyocyte normal behavior.

Calcium dynamics models of the cardiomyocyte have been developed in two ways. One based on a complete description of the chemical activities of the cellular elements, without voltage dependencies (Tang & Othmer, 1994; Hamam *et al*. 2000; Rocaries *et al*. 2004) and the other based on space variations in the cardiomyocyte, without the use of detailed chemical descriptions (Michailova *et al*. 2002). In any case, these models do not provide a prediction of the membrane potential and its interdependence with the calcium homeostasis.

The model presented in this paper contains a complete description of the cardiomyocyte, both calcium dynamics and electrical phenomena. It is based on the analysis of the cardiac muscle cell as a system of two interconnected continuous-stirred tank chemical reactors, and it accounts for the different mass transport mechanisms, the electrical phenomena and the chemical kinetics of the reactions taking place.

Along with the detailed description of the calcium dynamics and electrical phenomena related to the different cellular elements, some empirical structures are introduced in the model where dynamics are not completely understood. These elements will be finally tuned when adjusting the model to expert or experimental data. This "hybrid" formulation allows a certain compromise between precision and complexity of the model, and also helps to adapt it to different conditions.

In the following sections a formulation of the physical model proposed and the corresponding mathematical model

of the cardiac muscle cell are presented. Some simulations results allow the comparison of the model with previous ones. Validations with experimental data, after adapting the model to different species, are also included.

PHYSICAL MODEL

In order to express the interdependence between the electrical and the calcium dynamics, the cellular system is interpreted from a process-engineering point of view. Process systems (sub-systems) are defined to describe mass and energy transfer that occur in the boundaries between these sub-systems and the external space. Hence, the cell is represented as a system of two interconnected micro-chemical-reactors, namely the cytosol (or main reactor) and the sarcoplasmic reticulum (SR tank), as shown in Figure 1. The different transfer processes take place between these two sub-systems, and between them and the external medium, by means of different valves (L-channels and R-channels) and pumps (SERCA, sarcolemma pump and Na^{+}-Ca^{2+} exchanger). They are modeled using the principles of mass transfer, fluid-dynamics and the chemical kinetics of the reactions taking place in the system. In addition, the main reactor wall is electrically charged and its potential also modulates many of the chemical reactions involved.

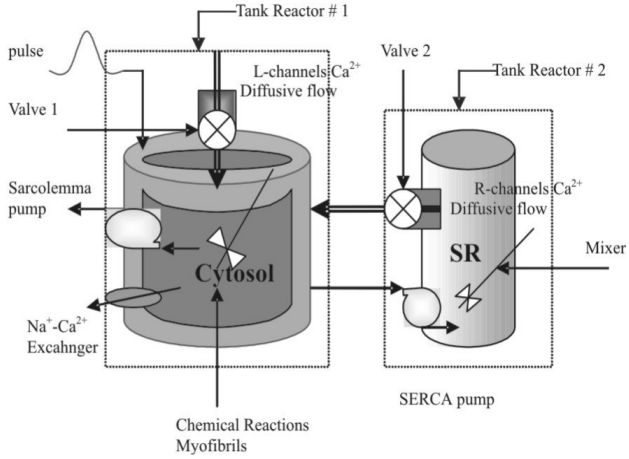

Figure 1. The cell as a system of interconnected reactors.

In order to formulate the mathematical equations of the model, it is assumed that:

-The cytosol and the sarcoplasmic reticulum are cylinders in spite of the particular distribution of the sarcoplasmic reticulum within a normal cardiomyocyte (Bray *et al*. 1994; Jafri *et al*. 1998; Fox *et al*. 2001).

-All chemical reactions occur in liquid phase (Tseng, 1988).

-Both tanks operate at constant volume, being the SR smaller than the cytosol. Volumes have been computed in previous works (Stern, 1992).

-The ionic concentrations are homogeneous throughout the cell, that is, there are not spatial concentration variations due to the very small size of the cardiomyocyte.

-There are no temperature gradients, therefore energy variations are neglected (Stern, 1992; Kargacin & Kargacin, 1997).

-The external membrane (sarcolemma) and the sarcoplasmic reticulum have the same transfer area.

-Extra-cellular concentrations of the different ions are constant (Stern, 1992).

-Variations in intracellular concentration of sodium and potassium ions are considered insignificant.

-Significant changes in voltage occur only in the cellular membrane or sarcolemma.

-An external pulse voltage signal triggers the depolarization of the sarcolemma and the calcium homeostasis.

-Calcium concentration and membrane potential are the principal actuators of the E-C coupling process.

MATHEMATICAL MODEL

The mathematical description of the system is based on the formulation of typical balance equations: mass balances both in the cytosol reactor and in the SR tank and a charge balance in the reactor wall.

Fundamental dynamic equations

Mass balance of calcium ion in the main reactor (cytosol):
Mass balances on other ions (potassium and sodium) are

$$V_{cyt}\cdot\frac{dCa_i^{2+}}{dt} = \\ = FD_{LC} + FD_{RC} - FQ_{ENa\text{-}Ca} + \\ - FQ_{SERCA} - FQ_{Sarcolema} + \\ - V_{cyt}\cdot\Sigma rR(V, Ca_i^{2+}, k_i)_i + \\ + V_{cyt}\cdot\Sigma rG(V, Ca_i^{2+}, k_i)_i \qquad (1)$$

Mass balance of calcium ion in the SR tank:

$$V_{SR}\cdot\frac{dCa_{SR}^{2+}}{dt} = FQ_{SERCA} - FD_{RC} \qquad (2)$$

not considered because of their faster dynamic response in relation to the calcium, as assumed above.

▪Charge balance in the main reactor wall:

Several ionic currents are produced because the ions tend to move from a region of high concentration to a region of low concentration, through the sarcolemma. Then the membrane can be seen as a conductor of electricity (ionic transport) with a conductance that may vary with changes in membrane potential (related to the opening of the membrane channels that allow the ionic transfer). Hence, the cellular membrane is an electrical circuit with resistance, capacitance, and charge or current (as in a battery). Current passes through the membrane either by charging the membrane capacity or by movement of ions through the ionic gates in parallel with the capacity. Thus there are mainly four ionic currents present in the cardiac muscle cell membrane: sodium current (I_{sodium}), calcium current ($I_{calcium}$), potassium current ($I_{potassium}$) and ionic-pumps current ($I_{ionicpumps}$). The equation representing this electrical phenomena is:
where:

$$\frac{dV}{dt} = -\frac{1}{C}\sum(I_{sodium} + I_{potassium} + I_{calcium} + I_{ionicpumps} + I_{stim}) \quad (3)$$

I_{stim} is the stimulus that triggers the membrane potential (square wave pulse).

Auxiliary equations

▪Diffusive flows:

Diffusive flows are produced by molecular transfer between regions of high and low ionic concentrations across the L-type channels (in the sarcolemma) and the Ryanodine channels or R-channels (in the SR membrane). Mathematical descriptions of these flows are obtained using Fick's law (Treybal, 1996), modulated by the fraction P of open channels:

$$J_A = -D_{AC} \cdot P \cdot \frac{C_{Ai} - C_{A0}}{l} \quad (4)$$

The activation of the protein that constitutes a channel, namely the conversion of the chemical reactions that changes the configuration of the protein to allow its opening may depend on the concentration of the present ions and on the membrane potential. Mass balances for the different transition states in the mechanisms of these reactions lead to the computation of the fraction P of open channels.

Ryanodine channels. According to Tang & Othmer (1994), the R-channels present four possible states:

- Activable (R): receptor empty.
- Open (RC^+): receptor with Ca^{2+} only on the positive site.
- Closed (RC^+C^-): receptor with Ca^{2+} on both positive and negative sites.
- Refractory (RC^-): receptor with Ca^{2+} on the negative site only.

▪The normalized variables are:

$$\frac{R}{R_T} = x_1 \quad (5)$$

$$\frac{RC^+}{R_T} = x_2 \quad (6)$$

$$\frac{RC^+C^-}{R_T} = x_3 \quad (7)$$

$$\frac{RC^-}{R_T} = x_4 \quad (8)$$

$$x_4 = 1 - x_1 - x_2 - x_3 \quad (9)$$

▪The mass balances related to each transition state are:

$$\frac{dx_1}{dt} = l_{-1} \cdot x_2 + l_{-2} \cdot (1-x_1-x_2-x_3) - (l_1+l_2) \cdot x_1 \cdot Ca_i^{2+} \quad (10)$$

$$\frac{dx_2}{dt} = -l_{-1} \cdot x_2 + l_{-2} \cdot x_3 + (l_1 \cdot x_1 - l_2 \cdot x_2) \cdot Ca_i^{2+} \quad (11)$$

$$\frac{dx_3}{dt} = -(l_{-2} + l_{-1}) \cdot x_3 + (l_2 \cdot x_2 + l_1 \cdot (1-x_1-x_2-x_3)) \cdot Ca_i^{2+} \quad (12)$$

▪Finally, the diffusive flow through the R-channels can be computed as:

$$FD_{RC} = D_{Ca^{2+}} \cdot x_2 \cdot \frac{Ca_{SR}^{2+} - Ca_i^{2+}}{l} \cdot A_{transf} \quad (13)$$

where:

x_2 is the fraction of open channels.

L-channels. Typically L-channels behavior is modeled using Hodgkin and Huxley theory (1952). Only three states of the channels are assumed, where the fraction *d* corres-

ponds to the open channels among the totality of channels in active state. The transformation rate that describes the behavior of fraction d is a simplified function of two parameters d^{∞} and τ_d, which are empirically adjusted using data from voltage-clamp experiments (Destexhe & Huguenard, 2000), and is obtained as:

$$\frac{dd}{dt} = \frac{d^{\infty} - d}{\tau_d} \qquad (14)$$

The diffusive flow due to the activity of the L-channels is given by:

$$FD_{LC} = D_{Ca^{2+}} \cdot d \cdot \frac{Ca_0^{2+} - Ca_i^{2+}}{l} \cdot A_{transf} \qquad (15)$$

▪ Chemical flows:

These flows are a result of the activity of the proteins called SERCA pump, sarcolemma pump and Na^+-Ca^{2+} exchanger, and are a function of the transport rate of each protein. This rate (reaction rate) is defined by the mechanisms of the chemical reactions involved in the calcium transfer. These processes are different from the transport through the R-channels and the L-channels since they occur against the concentration gradient.

SERCA pump. Using the simplification introduced by Tang & Othmer (1994); Hamam *et al*. (2000), that proposes a reaction mechanism of the Michaelis-Menten type (Michaelis & Menten, 1913), the reaction rate of the SERCA pump can be obtained as:

$$FQ_{SERCA} = \frac{p_1 \cdot \left(Ca_i^{2+}\right)^2}{p_2^2 + \left(Ca_i^{2+}\right)^2} \cdot V_{cyt} \qquad (16)$$

Sarcolemma pump. Is similar to the SERCA pump (Maclennan & Kranias, 2003), but its transport velocity is 90% slower (Negretti *et al*. 1995). Therefore the model by Tang & Othmer (1994) can be used changing the parameters as follows:

$$FQ_{Sarcolemma} = \frac{q_1 \cdot \left(Ca_i^{2+}\right)^2}{q_2^2 + \left(Ca_i^{2+}\right)^2} \cdot V_{cyt} \qquad (17)$$

where:

q_1: 0.1 times p_1.

q_2: 0.1 times p_2.

Na^+-Ca^{2+} exchanger: The kinetic mechanisms involved in the calcium flow induced by the Na^+-Ca^{2+} exchanger enzyme are not well understood, being the model by Michailova *et al*. (2002) the better alternative:

$$FQ_{ENa\text{-}Ca} = K \cdot \frac{1}{1 + \exp\left[\frac{-V}{V_{\max}}\right]} \cdot \frac{\left(Ca_i^{2+}\right)^n}{K_m^n + \left(Ca_i^{2+}\right)^n} \cdot V_{cyt} \qquad (18)$$

where:

the variable $V_{\max}$ is a discontinuous function of the voltage. To avoid problems in the numerical integration, a sigmoidal-type function is proposed to describe $V_{\max}$, as follows:

$$V_{\max} = K \cdot \frac{1}{1 + \exp\left[\frac{-V}{V_{\max}}\right]} \qquad (19)$$

▪Chemical reactions:

Calcium ions are produced or consumed by chemical reactions in the cytosol due to the activity of the myofibrils and the R-channels.

The myofibrils react with the calcium to produce their contraction-relaxation movement. This chemical activity has been described with a buffer-type mechanism as in Jafri and co-workers (1998), Fox *et al*. (2001) and Peskoff & Langer (1998). Hence the rates of generation (rG_{Miof}) and removal (rR_{Miof}) of calcium in the cytosol are given by:

$$rG_{Miof} = k_{d2} \cdot CaM \qquad (20)$$

$$rR_{Miof} = k_{d1} \cdot Ca_i^{2+} \cdot M \qquad (21)$$

The dynamical variations in the concentrations of myofibrils M and transition molecule CaM, must also be described in the model. The corresponding mass balances are:

$$\frac{dM}{dt} = - k_{d1} \cdot M \cdot Ca_i^{2+} + k_{d2} \cdot CaM \qquad (22)$$

$$\frac{dCaM}{dt} = k_{d1} \cdot M \cdot Ca_i^{2+} - k_{d2} \cdot CaM \qquad (23)$$

Finally, the total terms of calcium generation and removal in equation (1) are given by the following expressions, where the contributions of the activity of the R-channels have already been added:

$$\sum rG\left(V, Ca_i^{2+}, k_i\right)_i = = k_{d2} \cdot CaM + l_{-1} \cdot x_2 \cdot R_T + l_{-2} \cdot x_3 \cdot R_T + l_{-1} \cdot x_3 \cdot R_T + + l_{-2} \cdot (1 - x_1 - x_2 - x_3) \cdot R_T \qquad (24)$$

$$\sum rR\left(V, Ca_i^{2+}, k_i\right)_i = = k_{d1} \cdot Ca_i^{2+} \cdot M + l_1 \cdot x_1 \cdot Ca_i^{2+} \cdot R_T + l_{-2} \cdot x_3 \cdot R_T + l_{-1} \cdot x_3 \cdot R_T + + l_{-2} \cdot (1 - x_1 - x_2 - x_3) \cdot R_T \qquad (25)$$

▪Ionic currents in the sarcolemma:

The descriptions of the currents generated through the external wall of the cytosol (sarcolemma), namely, the sodium, potassium, calcium and ionic-pumps currents, are taken from the work by Fox *et al*. (2001), where the mathematical formulations are based on Ohm's law and Nerst-Plank's equation. We have used this work because their model improves the description of the electrical currents for the ventricular canine myocyte from the Luo and Rudy model, by means of the application of relatively simple mathematical equations that guarantee the obtaining of numerical rapid and stable solutions, quite unlike the model developed by Jafri *et al*. (1998).

Na^+ current: The activity of the sodium channels generates two kinds of sodium currents: I_{Na} that contributes to the fast depolarization of the sarcolemma (Bray *et al*. 1994; Jafri *et al*. 1998; Fox *et al*. 2001); I_{Nab} that is a small background current that contributes to action potential prolongation (Luo & Rudy, 1994):

$$I_{Na} = \bar{G}_{Na} \cdot m^3 \cdot h \cdot j \cdot (V - E_{Na}) \qquad (26)$$

$$I_{Nab} = \bar{G}_{Na} \cdot (V - E_{Na}) \qquad (27)$$

K^+-currents: Different fractions of the potassium channels produce different types of electric currents in the sarcolemma (Fox *et al*. 2001). The main potassium current is controlled by time-dependent and time-independent activation gates (Luo & Rudy, 1994), and is also well known as "the delayed rectifier potassium current". It is usually divided into two distinct currents I_{Kr} and I_{Ks}, which are distinguished by their kinetics (Winslow *et al*. 1999), and can be modeled (Luo & Rudy, 1994) as:

$$I_{Kr} = \bar{G}_{Kr} \cdot K_R \cdot K_{X_{Kr}} \cdot \sqrt{\frac{K_0^+}{4}} (V - E_K) \qquad (28)$$

$$I_{Ks} = \bar{G}_{Ks} \cdot K_{X_{Ks}}^2 \cdot (V - E_{Ks}) \qquad (29)$$

A background current (I_{K1}) is also present, over a wide range of potentials, and shows little time-dependence. It helps to maintain the resting potential of the cell and can be described as:

$$I_{K1} = \bar{G}_{Ks} \cdot K_1^{\infty} \cdot (V - E_K) \qquad (30)$$

The transient outward current I_{to}, is voltage and time dependent and is responsible of the fast early re-polarization phase of the action potential:

$$I_{to} = \bar{G}_{to} \cdot K_{X_{to}} \cdot K_{Y_{to}} \cdot (V - E_K) \qquad (31)$$

Finally, the plateau current (I_{Kp}) is the potassium contribution to plateau potential:

$$I_{Kp} = G_{Kp} \cdot K_{Kp} \cdot (V - E_K) \qquad (32)$$

Ca^{2+} currents: Three types of ionic currents are produced by the activity of the L-channels: I_{Ca}, I_{CaK} and I_{Cab}, with the following mathematical descriptions (Luo & Rudy, 1994; Jafri *et al*. 1998; Fox *et al*. 2001):

$$I_{Ca} = \bar{I}_{Ca} \cdot f \cdot d \cdot f_{Ca} \qquad (33)$$

$$I_{CaK} = \frac{\bar{P}_{CaK}}{C_{sc}} \cdot \frac{f \cdot d \cdot f_{Ca}}{1 + \frac{\bar{I}_{Ca}}{I_{Cahalf}}} \cdot \frac{1000 \cdot V \cdot F^2}{\Re \cdot T} \cdot \frac{K_i^{2+} \cdot \exp\left(\frac{2 \cdot V \cdot F}{\Re \cdot T}\right) - K_0^+}{\exp\left(\frac{2 \cdot V \cdot F}{\Re \cdot T}\right) - 1} \qquad (34)$$

$$I_{Cab} = \bar{G}_{Cab} \cdot (V - E_{Ca}) \qquad (35)$$

Ionic pump currents: The Na^+-Ca^{2+} exchanger, the Na^+-K^+ pump and the sarcolemma pump are located in the sarcolemma and their activity may modify the membrane potential. In fact these cellular elements are considered electrogenic (Luo & Rudy, 1994). Therefore three time-dependent currents are modelled: I_{NaK} (Na^+-K^+ pump), I_{NaCa} (Na^+-Ca^{2+} exchanger), and I_{pCa} (Sarcolemma pump):

$$I_{NaK} = \bar{I}_{NaK} \cdot f_{NaK} \cdot \frac{1}{1 + \left(\frac{K_{mNai}}{Na_i^+}\right)^{1.5}} \cdot \frac{K_0^+}{K_0^+ + K_{mKo}} \qquad (36)$$

$$I_{NaCa} = \frac{k_{NaCa}}{K^3_{mNa} + (Na_0^+)^3} \cdot \frac{\left[\exp\left(\frac{V \cdot F \cdot \eta}{\Re \cdot T}\right) \cdot (Na_i^+)^3 \cdot Ca_0^{2+} - \exp\left(\frac{V \cdot F \cdot (\eta - 1)}{\Re \cdot T}\right) \cdot (Na_0^+)^3 \cdot Ca_i^{2+}\right]}{K_{mCa} + Ca_0^{2+}} \cdot \frac{1}{1 + k_{sat} \cdot \exp\left(\frac{V \cdot F \cdot (\eta - 1)}{\Re \cdot T}\right)} \qquad (37)$$

$$I_{pCa} = \bar{I}_{pCa} \cdot \frac{Ca_i^{2+}}{K_{mpCa} + Ca_i^{2+}} \qquad (38)$$

GLOBAL STATE SPACE MODEL

The equations for the mass balances and main current are finally:

$$\frac{dCa_{SR}^{2+}}{dt} =$$

$$\left[- D_{Ca^{2+}} \cdot x_2 \cdot \frac{Ca_{SR}^{2+} - Ca_i^{2+}}{l} \cdot \frac{A_{transf}}{V_{cyt}} + \frac{p_1 \cdot (Ca_i^{2+})^2}{p_2^2 + (Ca_i^{2+})^2} \right] \cdot \frac{V_{cyt}}{V_{SR}} \quad (39)$$

$$\frac{dCa_i^{2+}}{dt} =$$

$$D_{Ca^{2+}} \cdot d \cdot \frac{Ca_0^{2+} - Ca_i^{2+}}{l} \cdot \frac{A_{transf}}{V_{cyt}} +$$

$$D_{Ca^{2+}} \cdot x_2 \cdot \frac{Ca_{SR}^{2+} - Ca_i^{2+}}{l} \cdot \frac{A_{transf}}{V_{cyt}} -$$

$$K \cdot \frac{1}{1 + \exp\left(\frac{-V}{V\max} \right)} \cdot \frac{(Ca_i^{2+})^n}{K_m^n + (Ca_i^{2+})^n} - \quad (40)$$

$$\frac{p_1 \cdot (Ca_i^{2+})^2}{p_2^2 \cdot (Ca_i^{2+})^2} - \frac{q_1 \cdot (Ca_i^{2+})^2}{q_2^2 \cdot (Ca_i^{2+})^2} +$$

$$k_{d2} \cdot CaM + l_{-1} \cdot x_2 \cdot R_T + l_{-1} \cdot x_3 \cdot R_T +$$

$$l_{-2} \cdot (1 - x_1 - x_2 - x_3) \cdot R_T + l_{-2} \cdot x_3 \cdot R_T -$$

$$k_{d1} \cdot Ca_i^{2+} \cdot M - l_{-1} \cdot x_1 \cdot Ca_i^{2+} \cdot R_T -$$

$$l_2 \cdot x_2 \cdot Ca_i^{2+} \cdot R_T - l_2 \cdot x_1 \cdot Ca_i^{2+} \cdot R_T -$$

$$- l_1 \cdot (1 - x_1 - x_2 - x_3) \cdot Ca_i^{2+} \cdot R_T$$

$$\frac{dV}{dt} = - \frac{1}{C} \left[\begin{array}{l} I_{Na} + I_{Nab} + I_{Kr} + I_{Ks} + I_{K1} + I_{to} + \\ I_{Kp} + I_{Ca} + I_{CaK} + I_{Cab} + I_{\mathrm{NaK}} + \\ I_{NaCa} + I_{pCa} + I_{stim} \end{array} \right] \quad (41)$$

Equations (39) to (41) allow the description of three output variables of the system: Ca_i^{2+}, Ca_{SR}^{2+} and V. The total formulation contains eighteen non-linear first order differential equations, since the integration of fifteen additional state-variables, namely d, x_1, x_2, x_3, M, CaM, m, h, j, $K_{X_{to}}$, $K_{Y_{to}}$, $K_{X_{Kr}}$, $K_{X_{Ks}}$, f and f_{Ca} is needed to solve the model. A first set of numerical values for the parameters is compiled, using data from different bibliographical sources, as shown in Table 1.

Table 1. Parameters of the model.

Parameter	Value	Parameter	Value
A_{transf}	1.58E-12 m^2	$\overline{P}_{Ca}$	226E-5 cm ms^{-1}
V_{cyt}	1.6E-14 m^3	$\overline{P}_{CaK}$	5.79E-5 cm ms^{-1}
V_{SR}	1.12E-15 m^3	$\overline{I}_{NaK\,\max}$	0.693 µA µF^{-1}
l	0.003E-6 m	I_{Cahalf}	-0.265 µA µF^{-1}
q_1	19 µMs^{-1}	$\overline{I}_{pCa\,\max}$	0.05 µA µF^{-1}
q_2	0.06 µM	η	0.35
K	150.3 µMs^{-1}	k_{sat}	0.2
K_m	1 µM	k_{NaCa}	1500 µA µF^{-1}
n	1	K_{mCa}	87.5 mM
k_{d1}	39 µM^{-1}s^{-1}	K_{mCa}	1380 µM
k_{d2}	20 s^{-1}	K_{mNai}	10 mM
l_1	15 µM^{-1}s^{-1}	K_{mKo}	1.5 mM
l_2	0.8 µM^{-1}s^{-1}	K_{mpCa}	0.05 µM
l_{-1}	7.6 s^{-1}	K_{mfCa}	0.18 µM
l_{-2}	0.84 s^{-1}	Na_0^+	138 mM
p_1	1038 µMs^{-1}	K_0^+	4 mM
p_2	0.12 µM	Ca_0^{2+}	2000 µM
$\overline{G}_{Na}$	12.8 mS µF^{-1}	Na_i^+	10 mM
$\overline{G}_{K1}$	2.8 mS µF^{-1}	K_i^+	149.4 mM
$\overline{G}_{Kr}$	0.0136 mS µF^{-1}	R_T	0.693 µA µF^{-1}
$\overline{G}_{Ks}$	0.003E-6 m	C_{sc}	-0.265 µA µF^{-1}
$\overline{G}_{Kp}$	19 µMs^{-1}	$D_{Ca^{2+}}$	0.05 µA µF^{-1}
$\overline{G}_{to}$	0.06 µM	F	0.35
$\overline{G}_{Nab}$	150.3 µMs^{-1}	R	0.2
$\overline{G}_{Cab}$	1 µM	T	310 K

SIMULATION

The initial conditions for the solution of the model are summarized in table 2.

Table 2. Initial Conditions.

Variable	Value	Variable	Value
t (s)	0	d	0.0001
V (mV)	- 94.7	f_{Ca}	0.942
Ca_i^{2+} (µM)	0.14	m	2.4676E-4
Ca_{SR}^{2+} (µM)	500	h	0.99869
M (µM)	70	j	0.99887
CaM (µM)	0	$K_{X_{Kr}}$	0.229
x_1	0.691	$K_{X_{Ks}}$	0.0001
x_2	0.192	$K_{X_{to}}$	3.742E-5
x_3	0.0254	$K_{Y_{to}}$	1
f	0.983		

The solver

The equations of the model are integrated with Simulink® of Matlab® (v6.5), using a variable-step numerical solver based on the algorithm by Klopfenstein (1971). This method is relatively fast and accurate, and allows the modification of the relative error tolerance and absolute error tolerance values (Shampine & Reichelt, 1997). The equipment used is a Pentium III 900MHz, 256MB RAM computer. The program takes 5 minutes to reproduce 40 minutes of cell cycles.

The validation procedure

The heuristic tuning of the model parameters allows an initial validation of a general model of the cardiac muscle cell, based on expert knowledge or typical experimental values for the dynamics of the output variables (Ca_i^{2+} and V). Specifically, validations are focused on:

Curb shapes: cyclic, with a plateau phase for V, and bell-shaped for Ca_i^{2+}.
Time periods: oscillation period for $V(t_{voltage})$ in the range 200-400 ms (Tseng, 1998), and oscillation period for Ca_i^{2+}, ($t_{calcium}$) in the range 800-1000 ms (Lecarpentier *et al.* 1996). Durations of the excitation and relaxation phases ($t_{exctcalcium}$ and $t_{relaxcalcium}$) of the calcium dynamic are also important, and frequently reported.
Maximum calcium gradient $\Delta_{calcium}$: oscillating between 0.8 and 1.1 μM (Lecarpentier *et al*. 1996).

The experimental data

Experimental data for validation is obtained from the literature and also from laboratory experiments.

Bibliographic sources

• Voltage V and current I_{Ca} for dog cardiomyocytes from the works of Winslow & Greenstein (2002); and for rabbit cardiomyocytes from the works of LI *et al.* (2002).
• Variable Ca_i^{2+} for human cardiomyocytes from Piacentino *et al.* (2003); and for dog cardiomyocytes from Winslow *et al.* (1999).

Laboratory data

An important amount of experimental data on Ca_i^{2+} in chicken cardiomyocytes has been collected at the Research Laboratory Unit 99 of the INSERM (Paris), based on quantitative calcium fluorescence. Detailed descriptions of the experimental protocols can be found in Hamam *et al*. (2000).

RESULTS AND COMPARISONS WITH PREVIOUS MODELS

It is interesting to remark that the model equations, and therefore the different sets of parameters, are associated with the different cellular elements. This type of information is summarized in Figure 2, where the different correspondences can be seen: Ryanodine channels to kinetic constants l_1,l_{-1}, l_2 and l_{-2}; SERCA pump to parameters p_1 and p_2; sarcolemma ATP-pump to parameters q_1 and q_2; Na^+-Ca^{2+} exchanger to parameters K, K_m, and n; myofibrilles activity to parameters k_{d1} and k_{d2}; and L-channels to kinetic constants d^∞ and τ_d.

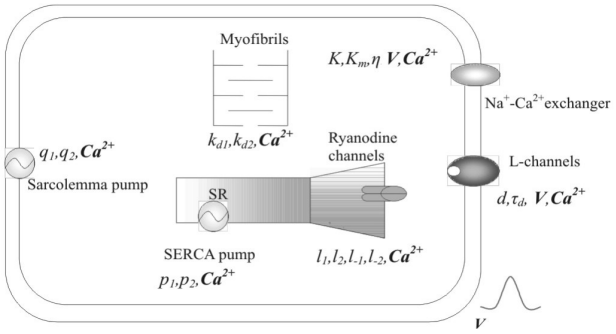

Figure 2. Cellular elements and corresponding model parameters.

With the aid of these relationships it is easy to accomplish the tuning of some parameters to make adjustments in the output responses of the model. Typical simulation results obtained after an initial parametric adjustment of the model (Table 3) are shown in Figures 3 and 4. The bell shaped curve for calcium dynamic and the plateau phase in voltage oscillations are observed as expected (Lecarpentier *et al*. 1996; Fabiato, 1985), with numerical values of $\hat{\Delta}_{calcium}$ =0.79 μM , $\hat{t}_{calcium}$ = 1 s and $\hat{t}_{voltage}$ =0.35 s which are similar to those reported in several bibliographic sources: $\Delta_{calcium}$ = 0.9 μM and $t_{calcium}$ =1 s (Berridge *et al*. 2003) and $t_{voltage}$ =0.4 s (Stern, 1992). The model is therefore able to represent a generalized mammal cardiomyocyte.

Table 3. Parameter tuning

Parameter	Value
$\overline{I}_{NaK}$	0.3465 μA μF^{-1}
p_1	10.38 μMs^{-1}
q_1	0.19 μMs^{-1}
K	120.24 μMs^{-1}
$D_{Ca^{2+}}$	0.678E -11 m^{2}s^{-1}

Figure 3 and 4 can also be used to compare the predictions of the proposed model to those obtained with the model by Tang & Othmer (1994) for calcium dynamic, and the model by Fox *et al.* (2001) for membrane potential. On one hand, the asymmetric form of the calcium curve and the value of $\hat{\Delta}_{calcium}$ are much more realistic than the results by Tang & Othmer (1994). Numerical results are reported on table 4.

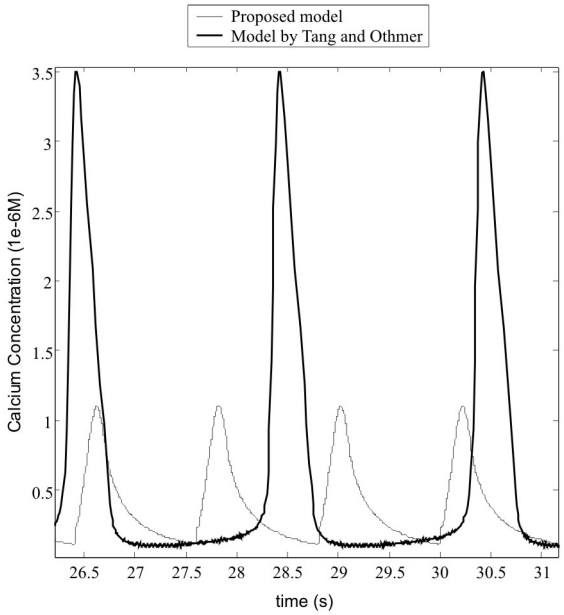

Figure 3. Generalizad cardiomyocyte calcium dynamics.

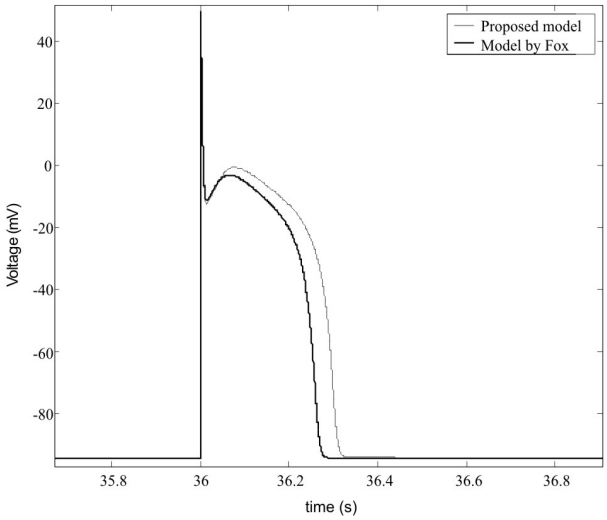

Figure 4. Generalizad cardiomyocyte voltage dynamics.

Table 4. Comparison of simulation results

		$\hat{t}_{calcium}$	$\hat{t}_{exctcalcium}$	$\hat{t}_{relaxctcalcium}$	$\hat{t}_{voltage}$	$\hat{\Delta}_{calcium}$
Model by Tang & Othmer (1994)	Value	2 s	1 s	1 s	-	3.3 μM
	$\varepsilon_{\%}$	100	233	43		267
Model by Fox *et al*. (2001)	Value	0.45 s	0.1 s	0.35 s	0.3 s	1.1 μM
	$\varepsilon_{\%}$	55	67	67	25	22
Proposed model	Value	1 s	0.2 s	0.8 s	0.35 s	0.79 μM
	$\varepsilon_{\%}$	0	33	14.29	12.5	12.22
Experimental Data	Value	1 s (Lecarpentier *et al*. 1996; Fabiato 1985)	0.3 s Fabiato, 1985)	0.7 s (Fabiato, 1985)	0.4 s (Stern, 1992)	0.9 μM (Fabiato, 1985)
	$\varepsilon_{\%}$					

On the other hand, the simulation of the membrane potential is very similar to the results of the model by Fox *et al.* (2001). Nevertheless, the latter produces a strange behavior when used to predict calcium dynamics (Figure 5), because it does not contain a detailed description of the calcium ion transport. In summary, the proposed model gives better results for prediction of the calcium dynamics, allowing the simultaneous simulation of the membrane potential with even better accuracy than the model by Fox *et al.* (2001).

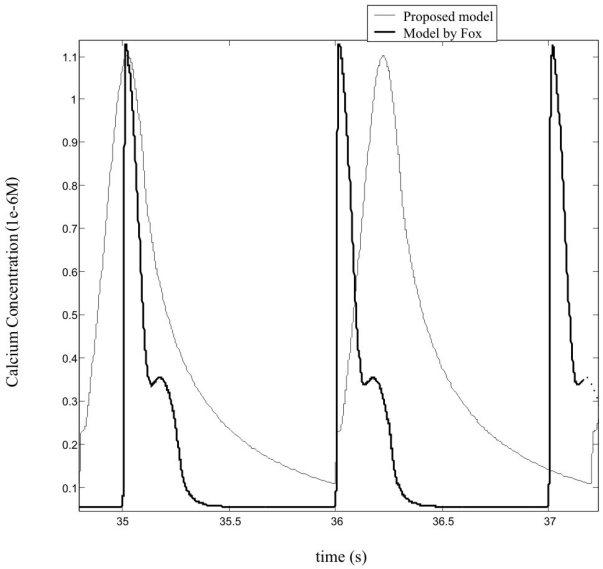

Figure 5. Generalizad cardiomyocyte calcium dynamics.

VALIDATIONS FOR DIFFERENT SPECIES

The model is now validated using different sets of experimental data, corresponding to cardiac muscle cells of different species. Occasionally, modifications of selected parameters are needed to adjust the model.

Canine cardiac cells

Experimental observations on canine cardiomyocytes (Winslow *et al.* 1999; Winslow & Greenstein, 2002) show that $t_{calcium}$=0.66 s, is substantially lower than the estimation of the generalized model ($\hat{t}_{calcium}$=1 s).

The following coefficients are changed to obtain this behavior:

i. Period of the input voltage pulse is increased to: a=0.6 s.
ii. Maximum transport rate K of the Na^+-Ca^{2+} exchanger is increased to K=1.6 μMs-1.

Figures 6 and 7 show the simulations of the calcium concentration and membrane potential dynamics obtained with the adjusted model, along with the experimental data. Numerical values of the main variables are reported on table 5 for comparison purposes.

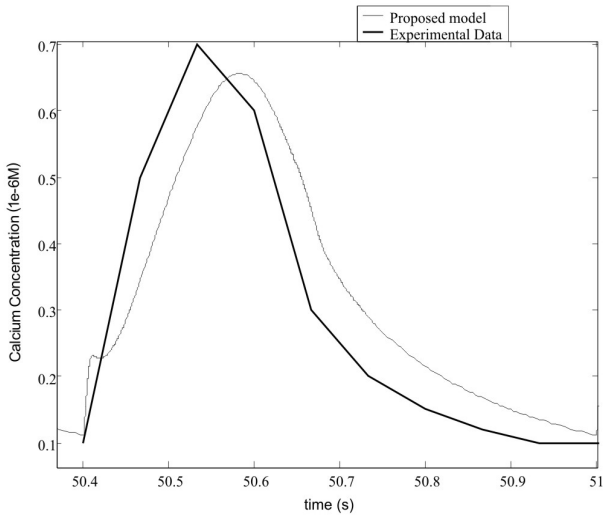

Figure 6. Ca_i^{2+} dynamics validation for canine cells.

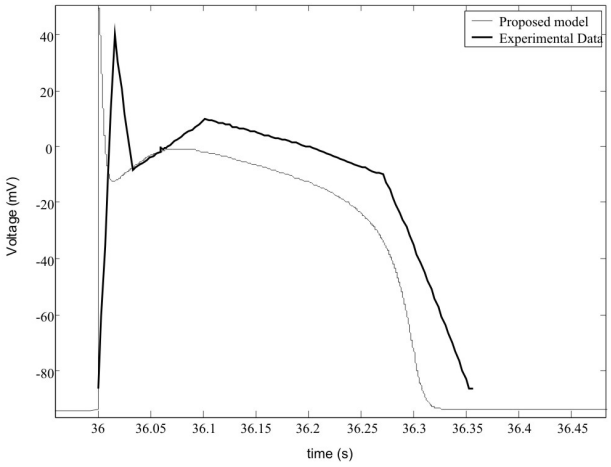

Figure 7. V dynamics validation for canine cells.

Rabbit cardiac cells

Li *et al*. (2002) report experimental data on the variables V and I_{Ca} for rabbit cardiac cells without further adjustments on the generalized model, the simulations show satisfactory results, as can be seen on Figures 8 and 9.

Chicken cardiac cells

Some parametric changes are needed in this case, to obtain the slower calcium dynamics that chicken cardiomyocytes show ($t_{calcium}$=1.85 s), namely:

i. Period of the input voltage pulse is increased to: a=1.8 s.

Table 5. Model validation for cells of different species.

	Canine cells	$\varepsilon_{\%}$	Rabbit cells	$\varepsilon_{\%}$	Chicken cells	$\varepsilon_{\%}$	Human cells	$\varepsilon_{\%}$
$t_{calcium}$ (s)	0.66	9.1	-		1.85	0.54	0.8	25
$\hat{t}_{calcium}$ (s)	0.6		1		1.84		1	
$t_{exctcalcium}$ (s)	0.15	33.33	-		0.35	11.43	-	
$\hat{t}_{exctcalcium}$ (s)	0.2		0.2		0.31		0.2	
$t_{relaxcalcium}$ (s)	0.41	2.44	-		1.55	1.29	-	
$\hat{t}_{relaxcalcium}$ (s)	0.4		0.8		1.53		0.8	
$t_{voltage}$ (s)	0.36	16.67	0.42	16.67	-		-	
$\hat{t}_{voltage}$ (s)	0.3		0.35		0.4		0.35	
$\Delta_{calcium}$ (μM)	0.6	8.33	-		1	5	0.8	1.25
$\hat{\Delta}_{calcium}$ (μM)	0.55		0.79		0.95		0.79	
$\Delta_{I_{Ca}}$ (μA)	-3.5	57.14	-0.75	100	-		-	
$\hat{\Delta}_{I_{Ca}}$ (μA)	-1.5		-1.5		-1.7		-1.5	

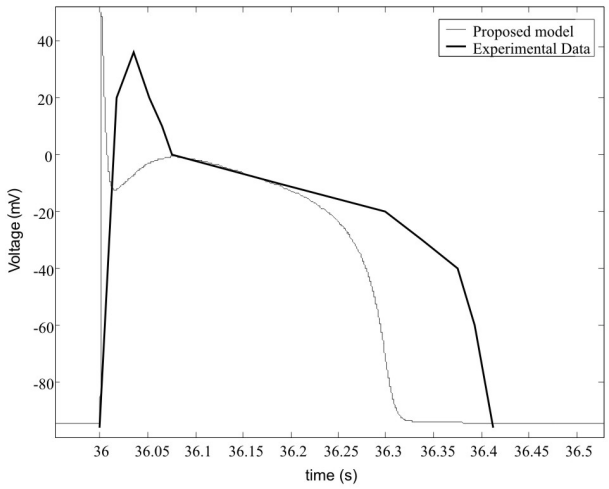

Figure 8. V dynamics validation for rabbit cells.

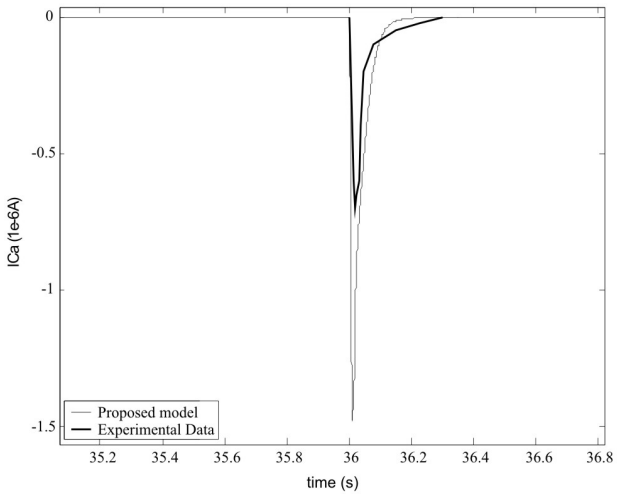

Figure 9. I_{Ca} dynamics validation for rabbit cells.

ii. The diffusion coefficient $D_{Ca^{2+}}$ is set to $D_{Ca^{2+}}$ = 0.658e-11 m^2/s.

Simulation results for calcium dynamics are very similar to experimental data, as can be seen in Figure 10 and table 5. Even if the membrane potential (Figure 11) cannot be validated due to the lack of voltage experimental data, it behaves as expected (in shape and duration: $\hat{t}_{voltage}$ =0.4 s. and $\hat{t}_{voltage} < t_{calcium}$).

Human cardiomyocytes

Few results on experiments with human cardiomyocytes are available. Data from Piacentino *et al*. (2003), that produce average values of $\Delta_{calcium}$=0.8 μM, and from Zhang *et al*. (2003), that indicate $t_{calcium}$=0.8 s, are used here for validation (Figure 12).

Validations have been extended to the simulation of other variables, namely Ca_{SR}^{2+}, x_2 and d. Even if experimental measurements of these variables are not available, the verification of the stability and the consistency of their behavior within the cell, helps to ensure the coherence of the model after the parametric adjustments.

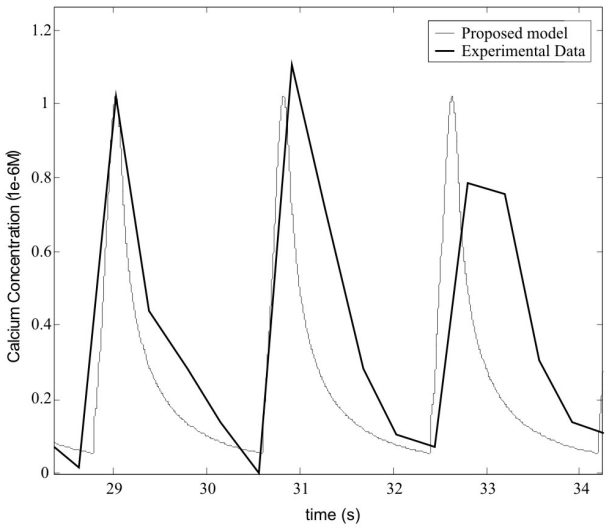

Figure 10. Ca_i^{2+} dynamics validation for chicken cells.

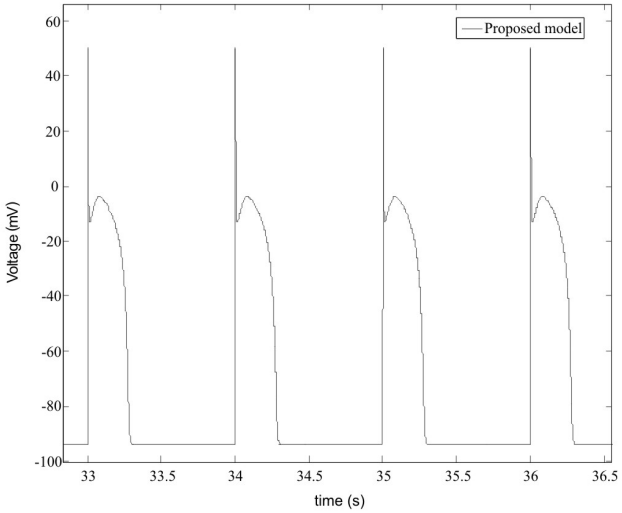

Figure 11. *V* dynamics simulation for chicken cells.

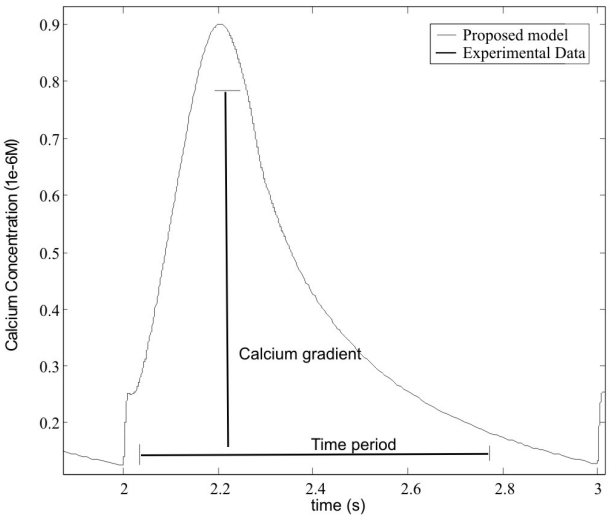

Figure 12. Ca_i^{2+} dynamics validation for human cells.

Figure 13 shows stable oscillations for the calcium concentration in the SR, Ca_{SR}^{2+}, with numerical values within the range from 60 μM to 500 μM as expected.

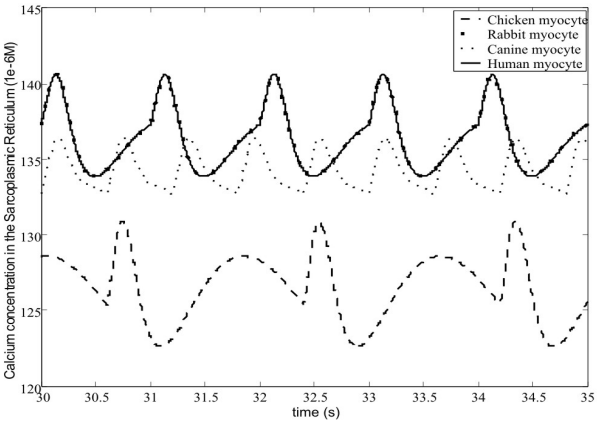

Figure 13. Sarcoplasmic reticulum. Simulation of Ca_{SR}^{2+}.

The dynamic behavior of the fraction of open Rianodine channels x_2, presented in Figure 14, is consistent with other results (Tang & Othmer, 1994; Hamam *et al*. 2000; Rocaries *et al*. 2004), and also shows values in the correct range (0-1).

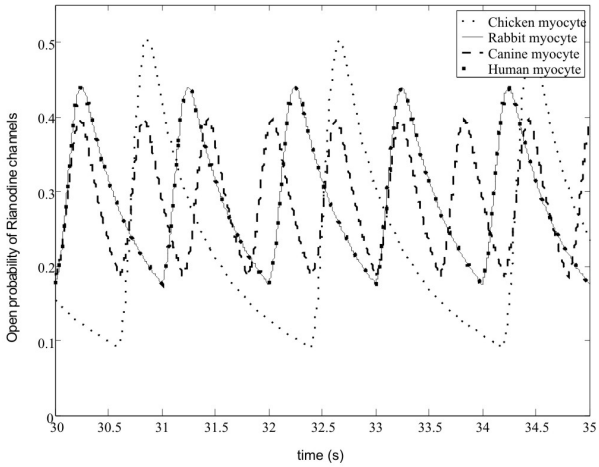

Figure 14. Rianodine channels. Simulation of x_2.

Similarly, for the fraction of open L-channels, *d*, stable cycles are observed, that oscillate between 0 and 1 (Figure 15). In all cases, *d* dynamics satisfactorily represents the sudden opening of the L-channels as a response to the initial voltage change, and their slow inactivation contributing to the plateau phase in the membrane potential.

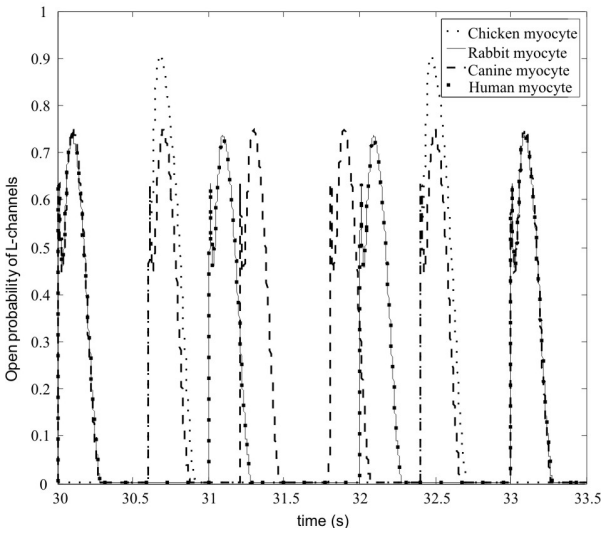

Figure 15. L-channels. Simulation of variable *d*.

CONCLUSIONS

A global model of the cardiac muscle cell has been presented in this paper. It provides calcium dynamics and electrical description of the cardiomyocyte, based on its interpretation as a two interconnected chemical reactors system.

Simulation results show that the model predicts the well-known cyclic behavior of the calcium concentration and the membrane potential of a cardiac muscle cell. Not only the shapes of the dynamic responses are accurate, but also the key numerical values are similar to experimental data (Table 5).

The formulation of the physical model as an integrated system of chemical reactors allows relating the calcium dynamics and electrical aspects of the cell dynamics, which has not been completely and coherently done in the past. Effectively, calcium and voltage predictions are more accurate than those obtained by previous models (Table 4).

Analyzing the summary of simulation results presented in Table 5, it can be said that a satisfactory validation of the model is achieved, except in very few situations. When prediction errors go beyond 15%, the possibility of structural errors in the model must be considered. However, since the basic phenomenological structure of the model allows relating parameters with cellular elements (Figure 2), the description of the cellular element involved in a certain type of alteration in the simulations can be improved.

Finally, a collateral result of the extensive validation procedures carried out in this paper, is an expert knowledge of the effects of different alterations in specific model components. Complete results of this sensitivity analysis, allowing the identification of the cellular elements that determine different kind of dynamic responses, will be presented in a companion paper. It is easy to foresee at this point the applications of the model to support pharmacological research for instance, because it can be used to study the effects of different drugs by determining which alterations in cellular elements produce certain pathological behaviors of the cell.

ACKNOWLEDGEMENTS

The work presented in this paper is the result of the French-Venezuelan collaboration research project entitled: “Modeling of the cardiac phenomena: from the cell to the organ”. The authors gratefully acknowledge the financial support of ECOS Nord (France), FONACIT, Universidad Simón Bolívar and FUNDAYACUCHO (Venezuela).

REFERENCES

Berridge, M., Bootman, M., Roderick, H. (2003). Calcium Signalling: Dynamics, Homeostasis and Remodelling. Nature Reviews 4; 517-529.

Bray, D., Bruce, A., Lewis, J., Raff, M., Roberts, K., Watson, J. (1994). Molecular Biology of the Cell. New York Garland, United States of America.

Destexhe, A. & Huguenard, J. (2000). Nonlinear Thermodynamic Models of Voltage-Dependent Currents. J. Comput. Neurosci. 9; 259-270.

Fabiato, A. (1985). Time and calcium dependence of activation and inactivation of calcium-induced release of calcium from the sarcoplasmic reticulum of a skinned canine cardiac purkinje cell. J. Gen. Physiol. 85; 247-289.

Fox, J., MCharg, J., Gilmour, R. (2001). Ionic mechanism of electrical alternans. Am. J. Physiol. Heart. Circ. Physiol. 282; H516-H530.

Gavaghan, D., Garny, A., Maini, P., Kohl, P. (2006). Mathematical models in physiology. Phil. Trans. Roy. Soc. Lond. 364; 1099-1106.

Guyton, A. (1997). Tratado de Fisiología Médica. MacGraw-Hill, México, p. 700.

Hamam, Y., Pecker, F., Rocaries, F., Lorino, H., Pavoine, C., Natowicz, R. (2000). Identification and modelling of calcium dynamics in cardiac myocytes. SIMPRA 222; 01-14.

Hodgkin, A. & Huxley, A. (1952). A quantitative description of membrane current and its application to conduction and excitation in nerve. J. Physiol. 177; 500-544.

Iribe, G., Kohl P., Noble, D. (2006). Modulatory effect of calmodulin-dependent kinase II (CaMKII) on sarcoplasmic reticulum Ca2+ handling and interval-force relations: a modelling study. Phil. Trans. R. Soc. A. 364; 1107-33.

Jafri, M., Jeremy, J., Winslow, R. (1998). Cardiac Ca2+ Dynamics: The Roles of Ryanodine Receptor adaptation and Sarcoplasmic Reticulum load. Biophys. J. 74; 1149-1168.

Kargacin, M. & Kargacin, G. (1997). Predicted changes in concentrations of free and bound ATP and ADP during intracellular Ca2+ signaling. Am. J. Physiol. Cell. Physiol. 273; C1416-C1426.

Klopfenstein, W. (1971). Numerical differentiation formulas for stiff systems of ordinary differential equations. RCA Review , 32; 447-462.

Lecarpentier, Y, Coirault, C., Chemla, D. (1996). Régulation cellulaire et moléculaire de la contraction cardiaque. Méd. Thér. 2; 113-122.

Li, G., Zhang, M., Satin, L., Baumgarten, C. (2002). Biphasic effects of cell volume on excitation-contraction coupling in rabbit ventricular myocytes. Am. J. Physiol. Heart. Circ. Physiol. 282; H1270-H1277.

Luo, C. & Rudy, Y. (1994). A Dynamic Model of the Cardiac Ventricular Action Potential, Part I and II. Circ. Res. 74; 1071-1096; 1097-1113.

MAClennan, D. & Kranias, E. (2003). Phospholamban: A Crucial Regulator of Cardiac Contractibility. Nature Reviews 4; 566-577.

Michaelis, L. & Menten, M. (1913). Kinetik der Inventinwirkung. Biochem. Z. 49; 333-369.

Michailova, A., Delprincipe, F., Egger, M., Niggli, E. (2002). Spatiotemporal Features of Ca2+ Buffering and Diffusion in Atrial Cardiac myocytes with Inhibited Sarcoplasmic Reticulum. Biophys. J. 83; 3134-3151.

Negretti, N., Varro, A., Eisner, D. (1995). Estimate of net calcium fluxes and sarcoplasmic reticulum calcium content during systole in rat ventricular myocytes. J. Physiol. 502; 471-479.

Noble, D. (2002). Modelling the heart: insights, failures and progress. BioEssays 24; 1155-1163.

Peskoff, A. & Langer, A. (1998). Calcium Concentration and Movement in the Ventricular Cardiac Cell during an Excitation-Contraction Cycle. Biophys. J. 74; 153-174.

Piacentino, V., Weber, C., Chen, X., Weisser-Thomas, J., Margulies, K., Bers, D., Houser, S. (2003). Cellular Basis of Abnormal Calcium Transients of Failing Human Ventricular myocytes. Circ. Res. 92; 651-658.

Rocaries, F., Hamam, Y., Roche, R., Delgado, M., Lamanna, R., Pecker, F., Pavoine, C., Lorino, H. (2004). Calcium Dynamics in Cardiac myocytes: a model for drugs effect description. SIMPRA 12; 93-104.

Sakmann, B. & Neher, E. (1995). Single Channel Recording. Plenum, United States of America, p. 700.

Shampine, L. & Reichelt, M. (1977). The MATLAB ODE Suite. SIAM J. Scient. Comput. 18; 1-22.

Söderström, T. & Stoica, P. (1989). System Identification. Prentice Hall International, United Kingdom, p. 256.

Stern, M. (1992). Theory of excitation-contraction coupling in cardiac muscle. Biophys. J. 63; 497–517.

Tang, Y. & Othmer, H. (1994). Model of Calcium Dynamics in Cardiac myocytes Based on the Kinetics of Ryanodine-Sensitive Calcium Channels. Biophys. J. 67; 2223-2235.

Treybal, R. (1996). Mass Transfer and Applications. MacGraw-Gill, United States of America, p. 118-140.

Tseng, G. (1988). Calcium current restitution in mammalian ventricular myocytes is modulated by intracellular calcium. Circ. Res. 63; 468–482.

Tusscher, K. & Panfilov, A. (2006). Alternans and spiral breakup in a human ventricular tissue model. Am. J. Physiol. Heart. Circ. Physiol. 291; H1088-H1100.

Winslow, R. & Greestein, J. (2002). Regulation of Action Potential Duration in a Ventricular Myocyte Model Incorporating Local-Control of JSR Ca2+ Release. [On line], Satellite Symposium of the Japanese BME Society http://www.cmbl.jhu.edu.

Winslow, R., Rice, J., Jafri, S., Marban, E., O'Rourke, B. (1999). Mechanisms of altered excitation-contraction

coupling in canine tacycardia - induced heart failure II: model studies. Circ. Res. 84; 571-586.

Zenglan, L. (2001). *Computation of excitation and propagation in inhomogeneous mammalian ventricular tissue*. Extracted [on line] on 2007 from: http://www.cs.ucla.edu/˜abingcao/lizzie/lizzie.html

Zhang, H., Noble, D., Cannell, M., Orchard, C., Lancaster, M., Jones, S., Boyett, M., Holden, A., Jafri, M., Sobie, E., Lederer, W., Demir, S., Michailova, A., Delprincipe, F., Egger, M., Niggli, E., Smith, G., Loughrey, C., MacQQuaide, N., Dempster, J., Trafford, A. (2003). *Dynamics of Cardiac Intracellular Ca^{2+} Handling From Experiments to Virtual Cells*. Int. J. Bif. Chaos. 13; 3535-3560.

NOMENCLATURE

$\Delta_{calcium}$: Maximum calcium gradient.

$\hat{\Delta}_{calcium}$: Maximum calcium gradient estimated by the model.

η: Correction factor for the Na+-Ca2+ exchanger current.

$\Re$: Ideal gas constant.

τ_d : L-channel kinetic constant.

$\sum rG(V, Ca_i^{2+}, k_i)_i$: Sum of generation rate of Ca^{2+} by chemical reactions.

$\sum rR(V, Ca_i^{2+}, k_i)_i$: Sum of removal rate of Ca^{2+} by chemical reactions.

a : Period of input voltage pulse.

A_{transf}: Transfer area of (sarcolemma or sarcoplasmic reticulum) membrane.

C : Cell membrane capacitance.

Ca_0^{2+} : Extra-cellular calcium concentration.

Ca_i^{2+} : Cytosol calcium concentration.

Ca_{SR}^{2+} : Sarcoplasmic reticulum calcium concentration.

CaM : Calcium-myofibril complex concentration.

C_{sc} : Specific membrance capacity.

C_{Ai}, C_{A0} : Concentration of component A inside and outside the membrane.

d : Fraction of active channels among the open L-channels.

d^{∞} : L-channel kinetic constant.

$D_{Ca^{2+}}$: Diffusion coefficient of calcium into the cytosol.

D_{AC} : Diffusion coefficient of component A into the cytosol.

E_{Ca} : Calcium equilibrium potential.

E_K : Potassium equilibrium potential.

E_{Ks} : I_{Ks} equilibrium potential.

E_{Na} : Sodium equilibrium potential.

f : Fraction of channels among the open L-channels inactivated by voltage.

f_{Ca} : Fraction of channels among the open L-channels inactivated by calcium.

f_{NaK} : Voltage-dependent Na+-K+ pump current factor.

F : Faraday constant.

FD_{LC} : Diffusive flow of calcium through the L-channels.

FD_{RC} : Diffusive flow of calcium through the R-channels.

$FQ_{ENa\text{-}Ca}$: Flow of calcium through the Na^+-Ca^{2+} exchanger.

FQ_{SERCA} : Flow of calcium through the SERCA pump.

$FQ_{Sarcolema}$: Flow of calcium through the Sarcolemma pump.

$\overline{G}_{Cab}$: Peak calcium background current conductance.

$\overline{G}_{K1}$: Peak inward rectifier potassium current conductance.

$\overline{G}_{Kp}$: Peak plateau potassium current conductance.

$\overline{G}_{Kr}$: Peak rapid component of the delayed rectifier potassium current conductance.

$\overline{G}_{Ks}$: Peak slow component of the delayed rectifier potassium current conductance.

$\overline{G}_{Na}$: Peak sodium current conductance.

$\overline{G}_{Nab}$: Peak sodium background current conductance.

$\overline{G}_{to}$: Peak transient outward potassium current conductance.

h : Fraction of channels among the open sodium channels rapidly inactivated by voltage.

I_{Ca} : L calcium channels current.

$\overline{I}_{Ca}$: Maximum L calcium channels current.

I_{Cab} : Calcium background current.

I_{Cahalf} : L calcium channels current level that reduces by one-half.

I_{CaK} : Potassium current through the L calcium channels.

$I_{calcium}$: Calcium current.

$I_{ionicpumps}$: Ionic pumps currents.

I_{K1} : Inward rectifier potassium current.

I_{Kp} : Plateau potassium current.

I_{Kr} : Rapid component of the delayed rectifier potassium current.

I_{Ks} : Slow component of the delayed rectifier potassium current.

I_{Na} : Sodium channels current.

I_{Nab} : Sodium background current.

I_{NaCa} : Na^+-Ca^{2+} exchange current.

I_{NaK} : Na^+-K^+ pump current.

$\overline{I}_{NaK}$: Maximum Na^+-K^+ pump current.

I_{pCa}: Sarcolemma Ca^{2+} pump current.

$\overline{I}_{pCa}$: Maximum sarcolemmal calcium pump current.

$I_{potassium}$: Potassium current.

I_{sodium} : Sodium current.

I_{stim} : Stimulus current that triggers the membrane potential (square wave pulse).

I_{to} : Transient outward potassium current.

j : Fraction of channels among the open sodium channels slowly inactivated by voltage.

J_A : Diffusive flow of substance A.

k_{d1}, k_{d2} :Myofibril reaction kinetic constants.

k_i : Constants of kinetic reactions.

k_{NaCa} : Scaling factor for Na^+-Ca^{2+} exchanger current.

k_{sat} : Saturation factor for Na^+-Ca^{2+} exchanger current.

K : Na^+-Ca^{2+} exchanger maximum rate.

K_0^+ : Extra-cellular potassium concentration.

K_1^∞ : Fraction of channels among the open potassium channels responsible of inward rectifier potassium current (I_{K1}).

K_i^+ : Intra-cellular potassium concentration.

K_{Kp} : Fraction of channels among the open potassium channels responsible of plateau potassium current ( ).

K_m : Calcium half-saturation constant for Na^+-Ca^{2+} exchanger.

K_{mKo} : Potassium half-saturation constant for Na^+-K^+ pump current.

K_{mNa} : Sodium half-saturation constant for Na^+-Ca^{2+} exchanger current.

K_{mNai} : Sodium half-saturation constant for Na^+-K^+ pump current.

K_{mCa} : Calcium half-saturation constant for Na^+-Ca^{2+} exchanger current.

K_{mpCa} : Half-saturation constant for sarcolemma calcium pump current.

K_R : Fraction of channels among the open potassium channels instantly activated by voltage and responsible of rapid component of the delayed rectifier potassium current (I_{Kr}).

$K_{X_{Kr}}$: Fraction of channels among the open potassium channels quickly activated by voltage and responsible of rapid component of the delayed rectifier potassium current (I_{Kr}).

$K_{X_{Ks}}$: Fraction of channels among the open potassium channels slowly inhibited by voltage and responsible of slow component of the delayed rectifier potassium current (I_{Ks}).

$K_{X_{to}}$: Fraction of channels among the open potassium channels quickly activated by voltage and responsible of transient outward potassium current (I_{to}).

$\overline{K}_{Y_{to}}$: Fraction of channels among the open potassium channels slowly inhibited by voltage and responsible of transient outward potassium current (I_{to}).

l : cell membrane wide.

l_1, l_{-1}, l_2, l_{-2} : Ryanodine-channels kinetic reactions constants (TANG and OTHMER, 1994).

m : Fraction of active channels among the open sodium channels.

M : Myofibrils concentration.

n : Saturation coefficient for Na^+-Ca^{2+} exchanger ($n = 1$).

Na_0^+ : Extra-cellular sodium concentration.

Na_i^+ : Intra-cellular sodium concentration.

p_1 : SERCA pump maximum rate.

p_2 : Threshold SERCA pump concentration.

P : Fraction of open channels.

$\overline{P}_{Ca}$: L calcium channels permeability to Ca^{2+}.

$\overline{P}_{CaK}$: L calcium channels permeability to K^{+}.

q_1 : Sarcolemma pump maximum rate.

$\hat{q}_2$: Threshold sarcolemma pump concentration.

rGM_{iof} : Sum of generation rate of Ca^{2+} by myofibrils chemical reactions.

rR_{Miof} : Sum of removal rate of Ca^{2+} by myofibrils chemical reactions.

R_T : Ryanodine channels total concentration.

t : Time.

$t_{voltage}$: Duration of voltage cycle.

$\hat{t}_{voltage}$: Duration of voltage cycle estimated by the model.

$t_{calcium}$: Duration of calcium cycle.

$\hat{t}_{calcium}$: Duration of calcium cycle estimated by the model.

$t_{exctcalcium}$: Duration of excitation stage in calcium cycle.

$\hat{t}_{exctcalcium}$: Duration of excitation stage in calcium cycle estimated by the model.

$t_{relaxcalcium}$: Duration of relaxation stage in calcium cycle.

$t_{relaxcalcium}$: Duration of relaxation stage in calcium cycle estimated by the model.

T : Temperature.

V : Voltage.

V_{cyt} : Cytosol volume.

V_{max} : Maximum voltage modulating the Na^{+}-Ca^{2+} exchanger kinetic reaction rate

V_{SR} : Sarcoplasmic reticulum volume.

x_1 : Fraction of Ryanodine channels in the transition state R.

x_2 : Fraction of Ryanodine channels in the transition state RC^{+} (open channel).

x_3 : Fraction of Ryanodine channels in the transition state $RC^{+}C^{-}$.

x_4 : Fraction of Ryanodine channels in the transition state RC^{-}.